# Supporting Information

# Intercalative Conformations of the 14*R* (+)- and 14*S* (–)-*trans*-*anti*-DB[*a,l*]P-$N^6$-dA Adducts: Molecular Modeling and MD Simulations

*Yuqin Cai[1], Shuang Ding[1], Nicholas E. Geacintov[2,]* and Suse Broyde[1,]**

Department of [1]Biology and [2]Chemistry, New York University, New York, N.Y. 10003, U.S.A.

***Corresponding authors:** Nicholas E. Geacintov, nicholas.geacintov@nyu.edu and Suse Broyde, broyde@nyu.edu

**Running Title:** NER of DB[*a,l*]P-Adenine Adducts

**Keywords:** Nucleotide excision repair, conformational heterogeneity, dibenzo[*a,l*]pyrene, MD simulations

***MD computation protocols.*** Our computational protocols follow recommendations of the AMBER development team (http://amber.scripps.edu/tutorials/basic/tutorial1/section5.htm). First, the starting models were subjected to 50 steps of conjugate gradient energy minimization, using a distance dependent dielectric function with dielectric constant 4.0. Then each system was neutralized with 20 $Na^+$ counterions and solvated with explicit water using the LEAP Module of the AMBER 9 simulation package (*1*). A periodic rectangular box of TIP3P water (*2*) with 10.0 Å buffer was created around the DNA for each sequence. The Particle-Mesh Ewald (*3, 4*) method with 9.0 Å cutoff for the non-bonded interactions was used in subsequent energy minimizations and MD simulations.

Subsequently, 500 steps of steepest descent minimization followed by 500 cycles of conjugate gradient minimization were conducted for the waters and counterions with 500 $kcal \cdot mol^{-1} \cdot Å^{-2}$ restraint on the DNA. Then, 500 steps of conjugate gradient minimization were carried out for the whole system without restraints. A 2.0 fs time step and the SHAKE algorithm (*5*) were applied in the MD simulations. All other parameters were default values in the AMBER 9 simulation package. The system was heated from 0 K to 300 K over 20 ps with the DNA fixed with a weak restraint of 10.0 $kcal \cdot mol^{-1} \cdot Å^{-2}$ at constant volume, using the Berendsen coupling algorithm (*6*) with a 1.0 ps coupling parameter. A 60 ps of constant pressure dynamics at 300 K followed to further equilibrate the system. Finally, a 30.0 ns production was conducted at a temperature of 300 K and constant pressure of 1 Atm. Temperature and pressure coupling constants were both 1.0 ps.

***Best representative structures.*** The best representative structure in the MD trajectory for each adduct was obtained by using the cluster analysis option in MOIL-View (*7*). The best representative structure is a real frame from the ensemble; as determined by a cluster analysis, it is the most populated conformation or the conformation that is the closest to all other snapshots in an ensemble.

***Hydrogen bond quality index analyses.*** We employed our hydrogen bond quality index (HBI) (*8*), to quantitatively assess the quality of Watson-Crick hydrogen bonding, in terms of the deviation from ideal Watson-Crick hydrogen bond distances and angles:

$$I_H = \sum_{D-H...A} [(d_{DA} - d_{DA}^0)^2 + (1 + \cos\gamma)^2]$$

where $d_{DA}$ is the instantaneous donor-acceptor distance, $d_{DA}^0$ is an ideal donor-acceptor distance (*9*) [O6 (G) to N4 (C) is 2.91 Å, N1 (G) to N3 (C) is 2.95 Å, and N2 (G) to O2 (C) is 2.86 Å] and $\gamma$ is the instantaneous donor-hydrogen···acceptor (D-H···A) hydrogen bond angle with an ideal value of 180 °. The summation is over all the Watson-Crick hydrogen bonds in a base pair over the trajectory. The lower the value of $I_H$, the better the quality of the Watson-Crick hydrogen bonding. $I_H$ is zero when the Watson-Crick hydrogen bonding is ideal during the dynamics. However, in real, even unmodified DNA, sequence-dependent deviations from ideal Watson-Crick hydrogen bonding are normal (*10*). Therefore, comparing the $I_H$ value of a modified step to its analogue step in the unmodified control duplex provides an estimate of the perturbation of its Watson-Crick hydrogen bond upon modification.

**Table S1. Ensemble average values with standard deviations (given in parentheses) for structural properties at the lesion site.**

| | *14R* (+) | *14S* (–) | Unmodified | |
|---|---|---|---|---|
| **Buckle** (°) | –26.4 (7.9) | 28.2 (7.5) | 4.4 (11.1) | |
| **Propeller** (°) | 21.4 (8.9) | –24.5 (7.6) | –6.8 (9.1) | |
| $\alpha'$ [a] (°) | –13.7 (8.4) | 15.6 (7.8) | N/A | |
| $\beta'$ (°) | 103.6 (7.7) | –100.9 (7.2) | N/A | |
| $\gamma'$ (°) | –62.7 (4.9) | 61.5 (5.3) | N/A | |
| $\delta'$ (°) | 24.2 (6.2) | –23.3 (6.4) | N/A | |
| **Twist** (°) | 17.1 (8.5) | –6.6 (10.7) | 32.0 (5.4) | |
| **Roll** (°) | 2.9 (8.9) | 23.6 (7.1) | –4.2 (6.9) | |
| **Rise (Å)** | 7.6 (0.4) | 7.1 (0.4) | 3.3 (0.5) | 3.4 (0.4) |
| **Tilt** (°) | –10.5 (5.7) | –16.0 (4.4) | 0.4 (5.7) | 1.8 (5.1) |
| **Opening (Å)** | 12.5 (8.0) | 11.3 (6.2) | 2.2 (6.2) | |
| $\chi$ (°) | –113.0 (18.9) | –58.0 (15.7) | –95.8 (29.5) | |
| **Total vdW interaction energy (kcal/mol) with the intercalation pocket** | –28.1 (1.7) | –25.0 (2.0) | N/A | |

[a] For $\alpha'$, we give the values for *R* and *S* as –13.7 (8.4) ° and 15.6 (7.8) °, respectively, to emphasize their inversion. These equal the respective values of 166.3 (8.4) ° and 195.6 (7.8) °, given in Figure S3, Supporting Information.

.

**Table S2. Ensemble average values of duplex helicoidal parameters with standard deviations (in parenthesis) for all cases. The steps highlighted in yellow are the ones where the lesion causes maximum distortion.**

| | 14*R* (+) | 14*S* (–) | Unmodified |
|---|---|---|---|
| | | **Twist (degrees)** | |
| **Step 3** | 27.9 (7.2) | 28.0 (5.1) | 30.3 (4.4) |
| **Step 4** | 16.1 (13.1) | 20.5 (7.3) | 36.9 (5.3) |
| **Step 5** | 34.2 (8.4) | 46.3 (8.0) | 23.9 (10.7) |
| **Step 6** | 17.1 (8.5) | –6.6 (10.7) | 32.0 (5.4) |
| **Step 7** | 28.9 (7.7) | 25.1 (5.8) | 34.3 (6.2) |
| **Step 8** | 34.9 (6.4) | 34.8 (6.5) | 32.8 (6.9) |
| **Step 9** | 28.2 (8.8) | 29.9 (8.2) | 29.1 (4.8) |
| | | **Roll (degrees)** | |
| **Step 3** | –0.8 (7.0) | –1.3 (5.5) | –2.9 (6.9) |
| **Step 4** | 1.0 (6.2) | 3.0 (5.4) | –1.6 (7.6) |
| **Step 5** | 8.1 (9.0) | –6.2 (6.3) | 10.5 (7.2) |
| **Step 6** | 2.9 (8.9) | 23.6 (7.1) | –4.2 (6.9) |
| **Step 7** | –4.7 (8.4) | –3.9 (7.9) | 2.1 (6.7) |
| **Step 8** | 4.7 (9.9) | 6.2 (11.1) | 3.4 (8.3) |
| **Step 9** | –3.3 (7.6) | –0.5 (6.8) | –10.6 (7.6) |
| | | **Buckle (degrees)** | |
| **Step 3** | –5.7 (10.8) | –4.6 (9.7) | –6.8 (10.5) |
| **Step 4** | 3.7 (9.2) | 5.3 (10.1) | –2.9 (10.9) |
| **Step 5** | 10.9 (10.3) | 16.9 (9.8) | –4.6 (11.4) |
| **Step 6** | –26.4 (7.9) | 28.2 (7.5) | 4.4 (11.1) |
| **Step 7** | –2.7 (10.6) | –10.5 (9.7) | 5.9 (10.3) |
| **Step 8** | 5.1 (11.1) | 3.8 (10.4) | –8.8 (11.8) |
| **Step 9** | –1.4 (12.6) | –0.7 (12.4) | –8.6 (11.4) |
| | | **Propeller (degrees)** | |

| | | | |
|---|---|---|---|
| **Step 3** | −11.4 (8.6) | −10.5 (8.6) | −13.9 (8.8) |
| **Step 4** | −10.9 (8.3) | −6.8 (8.2) | −13.8 (8.1) |
| **Step 5** | −13.8 (7.5) | −10.3 (8.1) | −6.1 (9.7) |
| **Step 6** | 21.4 (8.9) | −24.5 (7.6) | −6.8 (9.1) |
| **Step 7** | 8.2 (10.7) | 16.4 (8.6) | −13.4 (9.0) |
| **Step 8** | −12.6 (9.5) | −7.5 (9.5) | −21.1 (11.0) |
| **Step 9** | −13.6 (9.9) | −12.8 (9.5) | −7.2 (8.4) |
| | | **Opening (degrees)** | |
| **Step 3** | 1.5 (11.3) | 3.4 (5.4) | 3.9 (5.7) |
| **Step 4** | 0.2 (7.0) | 3.4 (5.6) | 1.4 (5.9) |
| **Step 5** | −2.0 (4.2) | 0.12 (3.7) | 1.6 (3.8) |
| **Step 6** | 12.5 (8.0) | 10.4 (6.0) | 2.2 (6.2) |
| **Step 7** | 2.7 (4.6) | 1.5 (6.3) | 1.4 (4.1) |
| **Step 8** | 0.9 (6.2) | 1.5 (6.3) | 9.4 (9.5) |
| **Step 9** | 4.1 (6.3) | 4.9 (5.8) | 0.6 (6.6) |
| | | **Rise (degrees)** | |
| **Step 3** | 3.2 (0.5) | 3.1 (0.3) | 3.2 (0.4) |
| **Step 4** | 3.3 (0.4) | 3.2 (0.3) | 3.4 (0.4) |
| **Step 5** | 7.6 (0.4) | 3.5 (0.3) | 3.3 (0.5) |
| **Step 6** | 3.0 (0.4) | 7.1 (0.4) | 3.4 (0.4) |
| **Step 7** | 3.3 (0.5) | 3.2 (0.3) | 3.6 (0.4) |
| **Step 8** | 3.5 (0.5) | 3.4 (0.4) | 3.2 (0.5) |
| **Step 9** | 3.2 (0.5) | 3.3 (0.5) | 2.9 (0.5) |
| | | **Tilt (degrees)** | |
| **Step 3** | 3.9 (6.3) | 1.3 (4.3) | 1.3 (5.1) |
| **Step 4** | 9.5 (5.7) | 3.4 (4.6) | 5.1 (6.0) |
| **Step 5** | −10.5 (5.7) | 8.5 (5.0) | 0.4 (5.7) |
| **Step 6** | 2.0 (4.6) | −16.0 (4.4) | 1.8 (5.1) |

| | | | |
|---|---|---|---|
| **Step 7** | 7.5 (5.6) | 0.0 (5.0) | 7.7 (6.4) |
| **Step 8** | 6.6 (7.1) | 3.1 (5.9) | 2.8 (7.0) |
| **Step 9** | 2.7 (8.9) | –0.3 (4.5) | 3.7 (6.6) |

**Table S3 (a). Ensemble average values with standard deviations (in parentheses) for minor groove widths (Å)**

| | **14*R* (+)** | **14*S* (−)** | **Unmodified** |
|---|---|---|---|
| **P6-P21** | 8.2 (3.5) | 6.9 (1.7) | 6.4 (1.6) |
| **P7-P20** | 10.8 (3.5) | 9.5 (1.5) | 7.2 (1.8) |
| **P8-P19** | 13 (1.7) | 12.6 (2.9) | 7.0 (1.5) |
| **P9-18** | 9.3 (1.9) | 12.1 (2.9) | 5.5 (1.5) |
| **P10-P17** | 7.2 (1.8) | 9.4 (1.9) | 6.3 (1.6) |
| **Total** | **48.5** | **50.5** | **32.4** |

**Table S3 (b). Ensemble average values with standard deviations (in parentheses) for major groove widths (Å)**

| | **14*R* (+)** | **14*S* (−)** | **Unmodified** |
|---|---|---|---|
| **P3-P17** | 17.2 (1.9) | 16.4 (1.6) | 14.4 (1.7) |
| **P4-P16** | 17.2 (1.5) | 18.7 (1.4) | 13.4 (2.0) |
| **P5-P15** | 16.8 (1.9) | 17.8 (1.9) | 14.5 (1.9) |
| **P6-P14** | 15.9 (1.7) | 17.6 (1.8) | 14.4 (1.9) |
| **Total** | **67.1** | **70.5** | **56.7** |

**Table S4 (a) Ensemble average values with standard deviations (in parentheses) for van der Waals interaction energies between adjacent base pairs and between DB[*a,l*]P and nearby base pairs [a]**

| Base pair step | Van der Waals interaction energy (kcal·mol$^{-1}$) | | |
|---|---|---|---|
| | **14*R* (+)** | **14*S* (–)** | **Unmodified** |
| **A3:T20-T4:A19** | –15.2 (1.3) | –15.5 (1.0) | –15.5 (0.9) |
| **T4:A19-C5:G18** | –14.9 (1.0) | –14.9 (1.0) | –14.9 (1.0) |
| **C5:G18-A6*:T17** | –1.4 (0.4) | –12.8 (1.0) | –14.5 (1.3) |
| **A6*:T17-C7:G16** | –14.3 (1.4) | –3.2 (0.6) | –15.6 (1.0) |
| **C7:G16-T8:A15** | –14.7 (1.1) | –14.4 (1.2) | –14.8 (1.0) |
| **T8:A15-A9:T14** | –13.9 (1.1) | –13.9 (1.1) | –14.2 (1.0) |
| **C5:G18-DB[*a,l*]P** | –15.0 (1.0) | –1.2 (0.1) | |
| **DB[*a,l*]P-A6*T17** | –12.0 (1.3) | –11.8 (1.3) | |
| **DB[*a,l*]P-C7:G16** | –1.1 (0.2) | –12.1 (1.6) | |
| **Total** | **–103** | **–99.8** | **–89.5** |
| **Difference between modified and unmodified duplexes** | **–13.5** | **–10.3** | |

[a] Only the aromatic rings are considered.

[b] Note that the ~3 kcal/mol difference between the 14*R* (+) and 14*S* (–) adducts is at the interactions highlighted in yellow.

**Table S4 (b) Ensemble average values with standard deviations (in parentheses) for van der Waals interaction energies (kcal·mol$^{-1}$) between the DB[*a,l*]P aromatic ring system and adjacent bases in the intercalation pocket** [a,b]

| | ***14R* (+)** | **14*S* (–)** |
|---|---|---|
| **DB[*a,l*]P-C5** | –5.5 (1.1) | –0.6 (0.1) |
| **DB[*a,l*]P-A6*** | –3.1 (1.1) | –2.9 (1.1) |
| **DB[*a,l*]P-C7** | –0.3 (0.1) | –2.2 (0.7) |
| **DB[*a,l*]P-G16** | –0.8 (0.2) | –9.8 (1.1) |
| **DB[*a,l*]P-T17** | –9.0 (0.7) | –8.9 (0.7) |
| **DB[*a,l*]P-G18** | –9.4 (1.0) | –0.5 (0.1) |
| **Total** | **–28.1 (1.7)** | **–25.0 (2.0)** |
| **DB[*a,l*]P-(A6* and T17)** [c] | –12.1 (1.3) | –11.8 (1.3) |

[a] Only the aromatic rings are considered.

[b] Note that the ~3 kcal/mol difference between the 14*R* (+) and 14*S* (–) adducts is at the interactions highlighted in yellow.

[c] Note that the entry DB[*a,l*]P-(A6* and T17) shows the interaction energies between the DB[*a,l*]P aromatic rings and the damaged base pair A6:T17 (Figures 6a and 6b), and are derived from the sum of DB[*a,l*]P-A6* and DB[*a,l*]P-T17.

**Table S5 (a) Hydrogen bond occupancies (%)** [a]

| | | **14*R* (+)** | **14*S* (–)** | **Unmodified** |
|---|---|---|---|---|
| **A3:T20** | N6-H61...O4 | 93.7 | 93.4 | 93.6 |
| | N3-H3...N1 | 99.4 | 95.3 | 99.3 |
| **T4:A19** | N3-H3...N1 | 98.6 | 96.6 | 97.6 |
| | N6-H62...O4 | 91.9 | 93.4 | 94.6 |
| **C5:G18** | N4-H41...O6 | 98.1 | 98 | 97.3 |
| | N2-H21...O2 | 99.9 | 99.4 | 99.7 |
| | N1-H1...N3 | 99.8 | 99.9 | 99.9 |
| **A6:T17** | N-HN...O4 | 95.6 | 97.7 | 95.2 |
| | N3-H3...N1 | 98.4 | 98.6 | 99.2 |
| **C7:G16** | N4-H41...O6 | 98.1 | 97.5 | 95.8 |
| | N2-H21...O2 | 99.3 | 99.5 | 99.4 |
| | N1-H1...N3 | 98.9 | 99.6 | 99.6 |
| **T8:A15** | N3-H3...N1 | 97.5 | 98.1 | 99.1 |
| | N6-H62...O4 | 96.4 | 95.3 | 79 |
| **A9:T14** | N6-H61...O4 | 90.7 | 90.2 | 96.6 |
| | N3-H3...N1 | 99.3 | 99.3 | 95.4 |
| **Extra HBs** | | | | |
| | O13-HO13...N7 (A6) | 92.6 | 30.6 | |
| | (C7)N4-H42...O12 | 68.9 | 45.0 | |

[a] Criteria for hydrogen bonding: heavy atom-heavy atom distance < 3.3 Å, and donor-hydrogen-acceptor angle > 140 °.

**Table S5 (b) Hydrogen bond quality for the Watson-Crick base pairs adjacent to the lesion site and their corresponding unmodified control base pairs.**

| HBI | *14R* (+) | 14*S* (–) | Unmodified |
|---|---|---|---|
| **C5:G18** | 318 | 321 | 343 |
| **A6:T17** | 375 | 397 | 416 |
| **C7:G16** | 357 | 956 | 390 |

**Table S6a. Partial charges, atom types and topologies for the 14*R* (+)- and 14*S* (–)-*trans-anti*-DB[*a,l*]P-$N^6$-dA adducts**

| | Atom name | Atom type | Topology | Partial charge | |
|---|---|---|---|---|---|
| | | | | **14*R* (+)** | **14*S* (–)** |
| 1 | P | P | M | 1.2553 | 1.2687 |
| 2 | O1P | O2 | E | –0.795 | –0.795 |
| 3 | O2P | O2 | E | –0.795 | –0.795 |
| 4 | O5' | OS | M | –0.477 | –0.476 |
| 5 | C5' | CT | M | –0.115 | –0.169 |
| 6 | H5'1 | H1 | E | 0.1096 | 0.1079 |
| 7 | H5'2 | H1 | E | 0.1096 | 0.1079 |
| 8 | C4' | CT | M | 0.2273 | 0.3142 |
| 9 | H4' | H1 | E | 0.1026 | 0.0639 |
| 10 | O4' | OS | S | –0.426 | –0.451 |
| 11 | C1' | CT | B | –0.029 | 0.2203 |
| 12 | H1' | H2 | E | 0.17 | 0.1191 |
| 13 | N9 | N* | S | –0.029 | –0.081 |
| 14 | C8 | CK | B | 0.03 | 0.1243 |
| 15 | H8 | H5 | E | 0.1868 | 0.1856 |
| 16 | N7 | NB | S | –0.405 | –0.661 |
| 17 | C5 | CB | S | 0.0547 | 0.0524 |
| 18 | C6 | CA | B | 0.3264 | 0.4648 |
| 19 | N | N2 | B | –0.245 | –0.535 |
| 20 | HN | H | E | 0.2853 | 0.3617 |
| 21 | C14 | CT | B | –0.014 | –0.025 |
| 22 | HC14 | H1 | E | 0.2105 | 0.1766 |

| | | | | | |
|---|---|---|---|---|---|
| 23 | C13 | CT | 3 | 0.0083 | 0.0299 |
| 24 | HC13 | H1 | E | 0.112 | 0.1574 |
| 25 | O13 | OH | S | −0.604 | −0.625 |
| 26 | HO13 | HO | E | 0.4232 | 0.3875 |
| 27 | C12 | CT | 3 | 0.1817 | 0.2376 |
| 28 | HC12 | H1 | E | 0.1019 | 0.0834 |
| 29 | O12 | OH | S | −0.662 | −0.659 |
| 30 | HO12 | HO | E | 0.4314 | 0.4245 |
| 31 | C11 | CT | 3 | 0.1404 | 0.1874 |
| 32 | HC11 | H1 | E | 0.0712 | 0.0222 |
| 33 | O11 | OH | S | −0.695 | −0.637 |
| 34 | HO11 | HO | E | 0.4424 | 0.4095 |
| 35 | C16 | CA | S | −0.041 | −0.019 |
| 36 | C10 | CA | B | −0.256 | −0.11 |
| 37 | HC10 | HA | E | 0.1545 | 0.134 |
| 38 | C17 | CA | B | 0.0666 | 0.0099 |
| 39 | C18 | CA | E | 0.0226 | 0.0406 |
| 40 | C9 | CA | B | −0.159 | −0.192 |
| 41 | HC9 | HA | E | 0.1338 | 0.1575 |
| 42 | C8 | CA | B | −0.226 | −0.216 |
| 43 | HC8 | HA | E | 0.1593 | 0.1477 |
| 44 | C20 | CA | B | 0.0519 | 0.0808 |
| 45 | C21 | CA | E | 0.1033 | 0.1306 |
| 46 | C7 | CA | B | −0.185 | −0.209 |
| 47 | HC7 | HA | E | 0.1499 | 0.1559 |
| 48 | C6 | CA | B | −0.169 | −0.207 |
| 49 | HC6 | HA | E | 0.1479 | 0.1425 |

| | | | | | |
|---|---|---|---|---|---|
| 50 | C5 | CA | B | −0.163 | −0.155 |
| 51 | HC5 | HA | E | 0.1521 | 0.1894 |
| 52 | C22 | CA | S | −0.019 | 0.0278 |
| 53 | C23 | CA | S | 0.0285 | 0.0635 |
| 54 | C4 | CA | B | −0.179 | −0.217 |
| 55 | HC4 | HA | E | 0.135 | 0.1477 |
| 56 | C3 | CA | B | −0.104 | −0.146 |
| 57 | HC3 | HA | E | 0.1313 | 0.1399 |
| 58 | C2 | CA | B | −0.153 | −0.146 |
| 59 | HC2 | HA | E | 0.1528 | 0.1255 |
| 60 | C1 | CA | B | −0.15 | −0.18 |
| 61 | HC1 | HA | E | 0.1249 | 0.1492 |
| 62 | C24 | CA | S | 0.0427 | 0.0454 |
| 63 | C19 | CA | S | −0.046 | −0.087 |
| 64 | C15 | CA | E | 0.0147 | −0.062 |
| 65 | N1 | NC | S | −0.753 | −0.702 |
| 66 | C2 | CQ | B | 0.6729 | 0.6403 |
| 67 | H2 | H5 | E | 0.0278 | 0.0355 |
| 68 | N3 | NC | S | −0.775 | −0.787 |
| 69 | C4 | CB | E | 0.4191 | 0.4804 |
| 70 | C3' | CT | M | 0.1698 | 0.2263 |
| 71 | H3' | H1 | E | 0.069 | 0.0398 |
| 72 | C2' | CT | B | −0.05 | −0.056 |
| 73 | H2'1 | HC | E | 0.0394 | 0.0257 |
| 74 | H2'2 | HC | E | 0.0394 | 0.0257 |
| 75 | O3' | OS | M | −0.472 | −0.467 |

**Table S6b. Added force field parameters** [a]

| Angle | $K_\theta$ (kcal·mol$^{-1}$·rad$^{-2}$) | $\theta_{eq}$ (deg) |
|---|---|---|
| N2-CT-CA | 80.0 | 111.20 |
| H1-CT-CA | 50.0 | 109.50 |
| OH-CT-CA | 50.0 | 109.50 |

[a] Missing angle parameters were added to the force field by analogy to chemically similar atom types already exist in the parm99 parameter set.

**Table S7. Box size and number of waters added to the MD simulation starting models**

| | **14*R* (+)** | **14*S* (–)** | **Unmodified** |
|---|---|---|---|
| **Box size (Å$^3$)** | 51 X 48 X 74 | 49 X 51 X 69 | 50 X 51 X 67 |
| **Number of waters added** | 4157 | 3911 | 3872 |

**(a)**

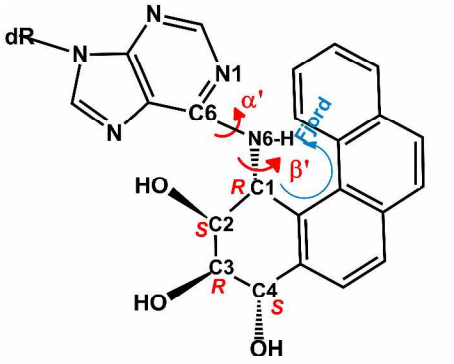


1*R* (+)-*trans-anti*-B[*c*]Ph-$N^6$-dA

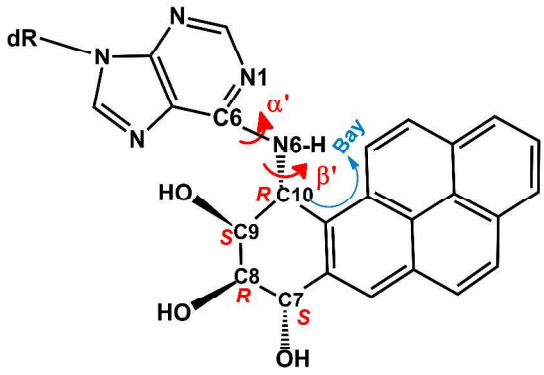


10*R* (–)-*trans-anti*-B[*a*]P-$N^6$-dA

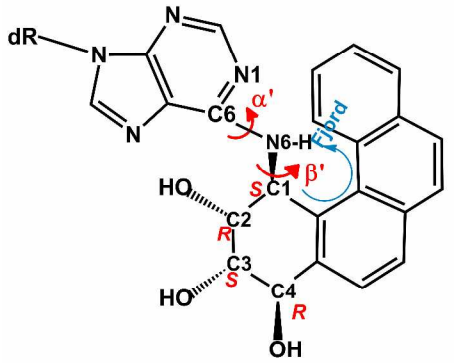


1*S* (–)-*trans-anti*-B[*c*]Ph-$N^6$-dA

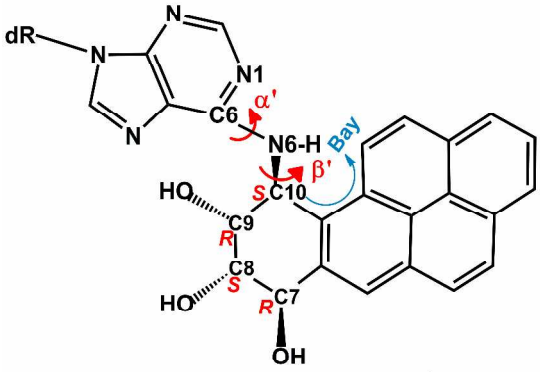


10*S* (+)-*trans-anti*-B[*a*]P-$N^6$-dA

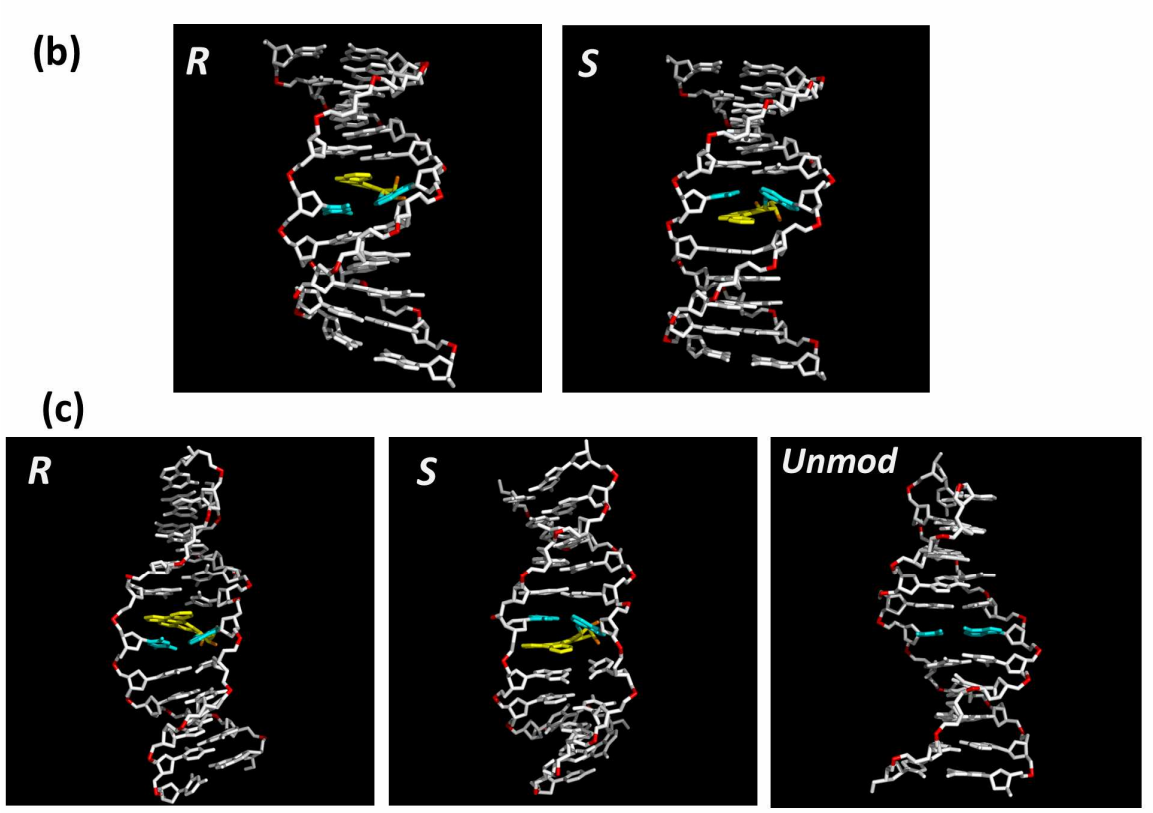


**Figure S1**. (a) Chemical structures of the 1*R* (+)- and 1*S* (−)-*trans-anti*-B[*c*]Ph-$N^6$-dA adducts as well as the 10*R* (−)- and 10*S* (+)-*trans-anti*-B[*a*]P-$N^6$-dA adducts. (b) NMR solution structures of the 11 mer duplexes for the 1*R* (+)- and 1*S* (−)-*trans-anti*-B[*c*]Ph-$N^6$-dA adducts (*11, 12*) (c) Best representative structures (*7*) of the 11 mer duplexes for the 14*R* (+)- and 14*S* (−)-*trans-anti*-DB[*a,l*]P-$N^6$-dA adducts, as well as the unmodified control (present work). Views are into the minor grooves.

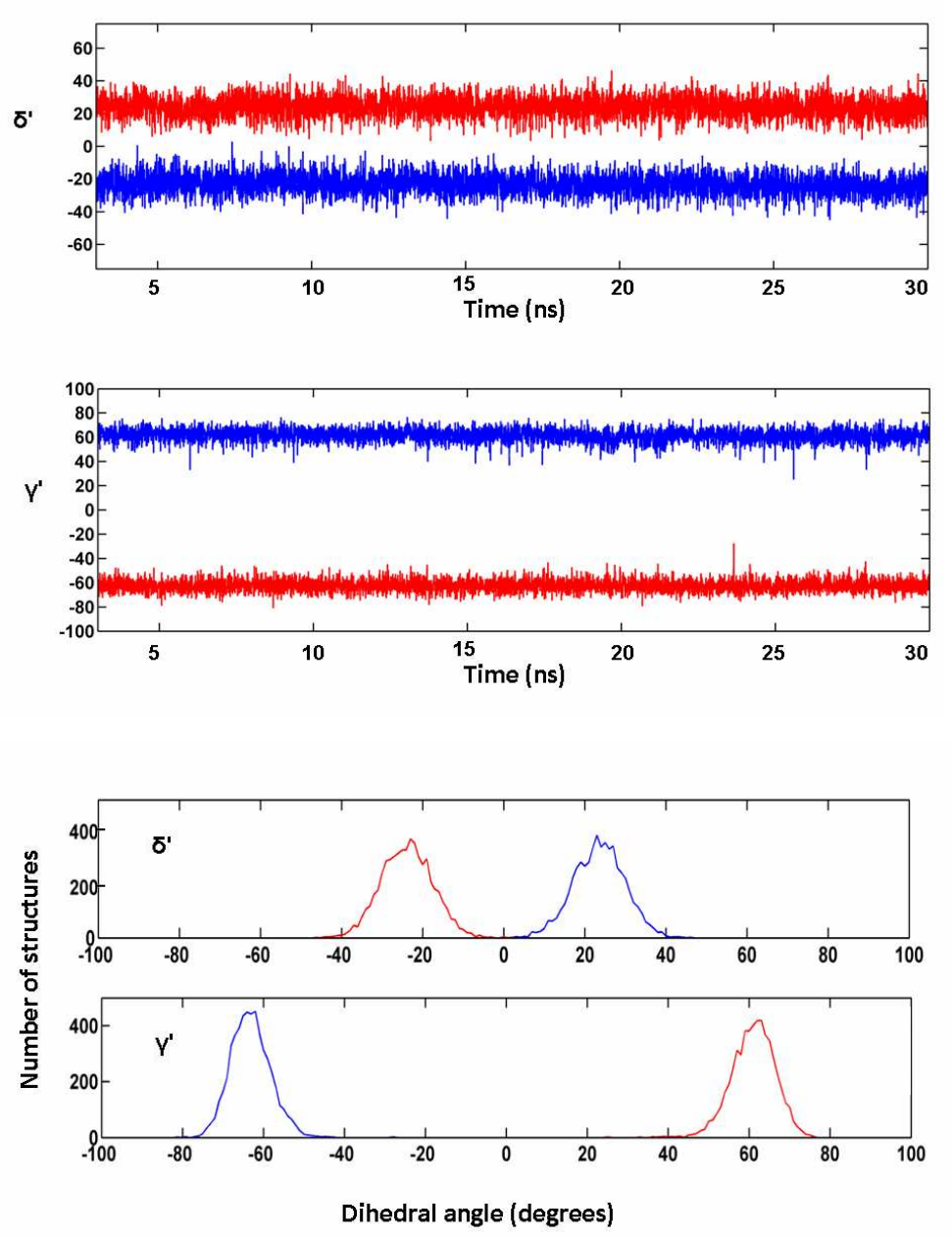


**Figure S2.** Time-dependence and population distribution of the fjord region twist angle δ′ and benzylic ring pucker torsion angle γ′. The 14*R* (+)-adduct is red, the 14*S* (–)-adduct is blue, and the unmodified control duplex is green. Means and standard deviations are given in Table S1.

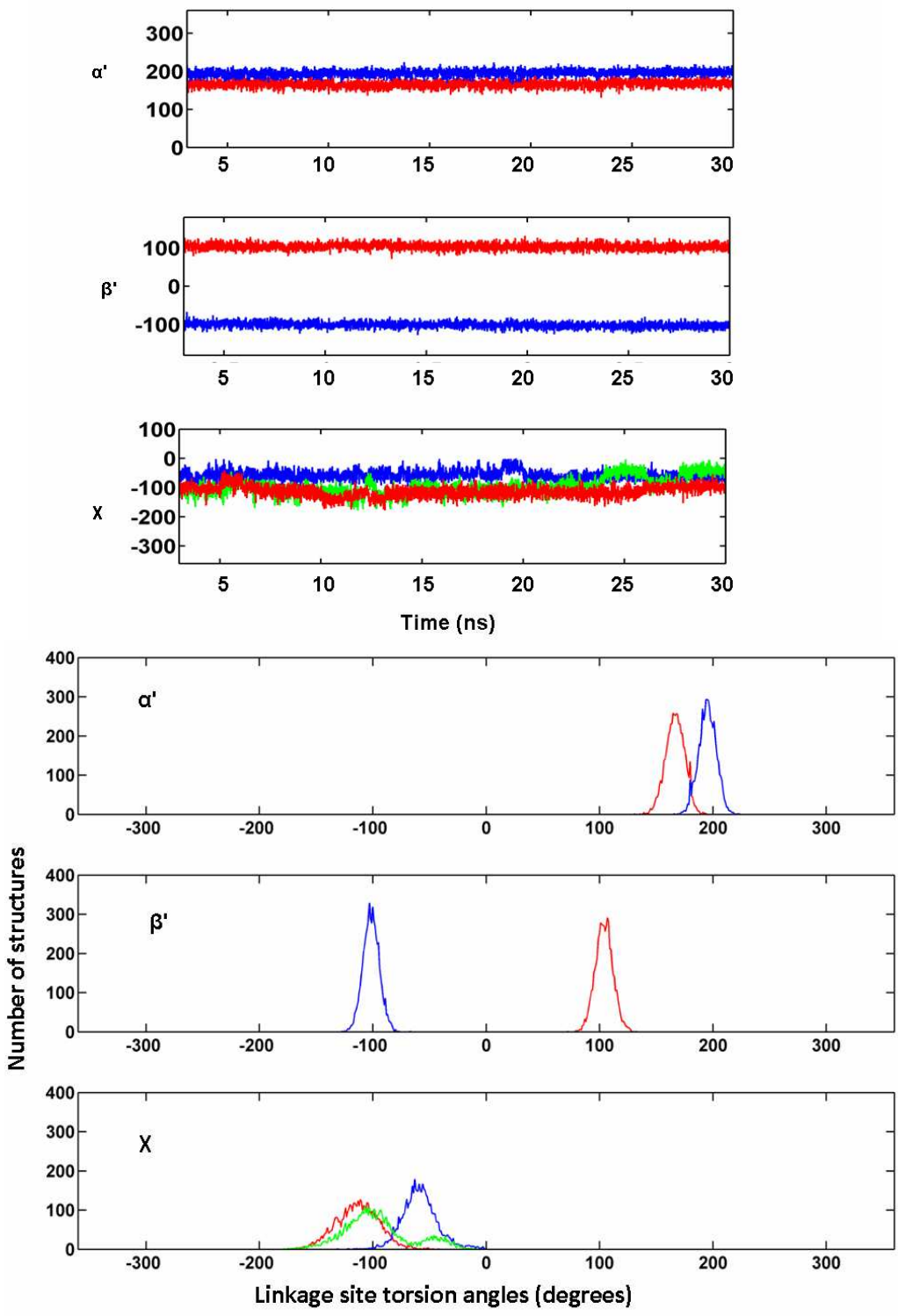


**Figure S3.** Time-dependence and population distributions of the carcinogen-DNA linkage site and glycosidic torsional angles α´, β´ and χ. The 14*R* (+)-*trans-anti*-DB[*a,l*]P-$N^6$-dA adduct is red, the 14*S* (–)-*trans-anti*-DB[*a,l*]P-$N^6$-dA adduct is blue, and the unmodified control duplex is green. Means and standard deviations are given in Table S1.

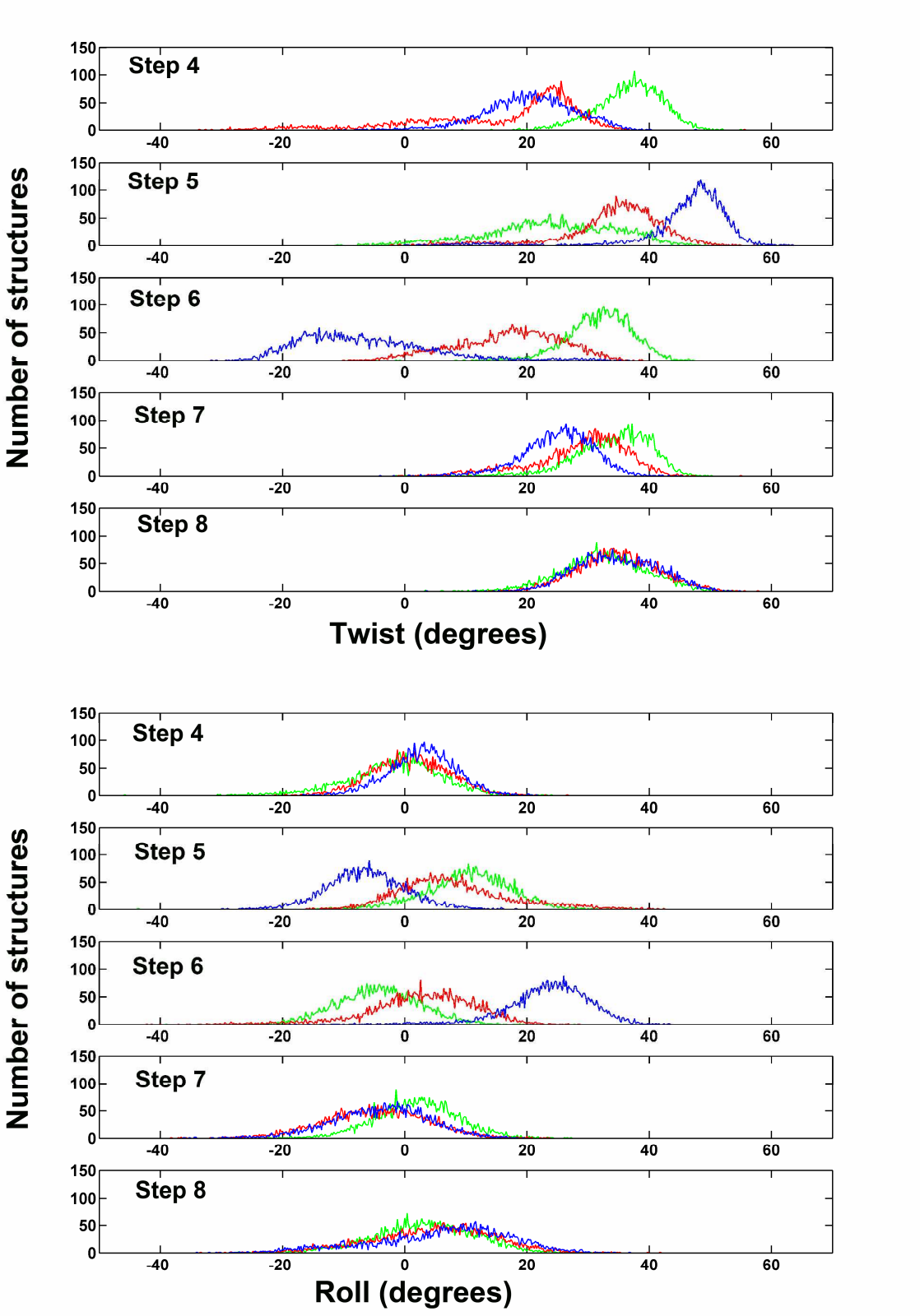
Step 4
Step 5
Step 6
Step 7
Step 8
Number of structures
Twist (degrees)
Step 4
Step 5
Step 6
Step 7
Step 8
Number of structures
Roll (degrees)

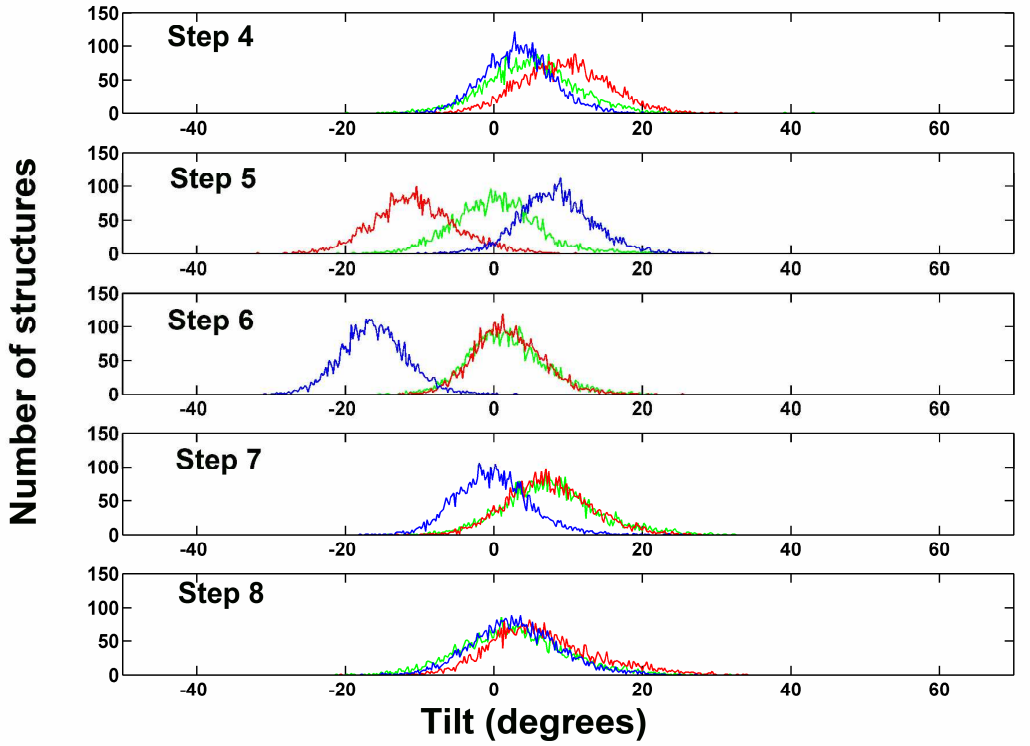
Step 4
Step 5
Step 6
Step 7
Step 8
Number of structures
Tilt (degrees)

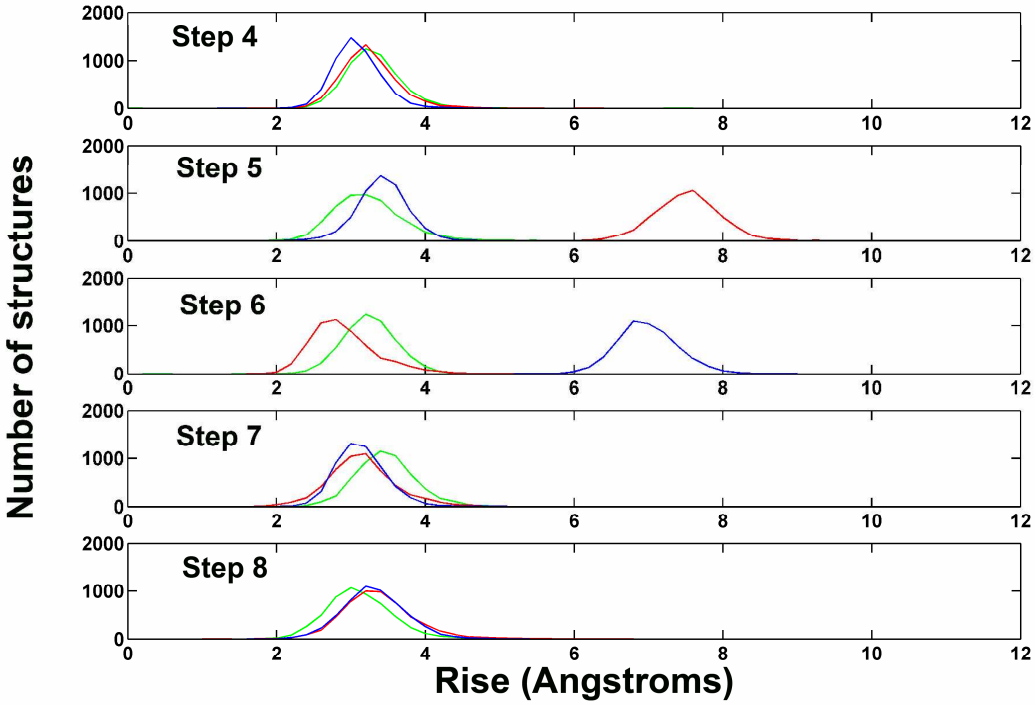
Step 4
Step 5
Step 6
Step 7
Step 8
Number of structures
Rise (Angstroms)

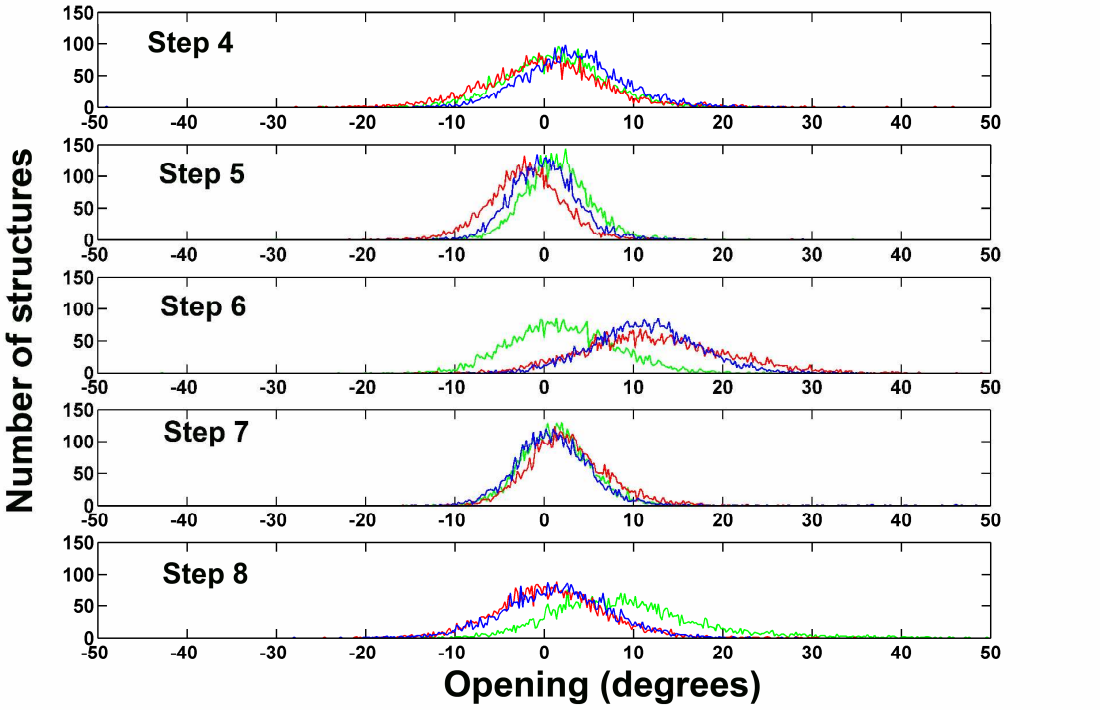
Step 4
Step 5
Step 6
Step 7
Step 8
Number of structures
Opening (degrees)

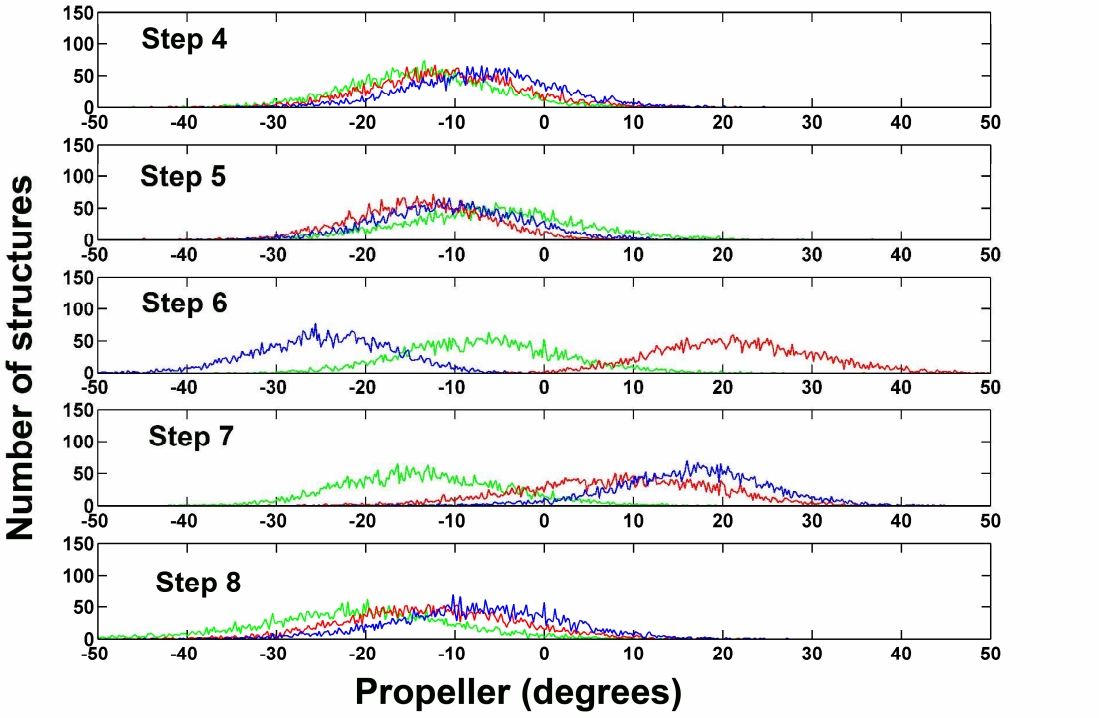
Step 4
Step 5
Step 6
Step 7
Step 8
Number of structures
Propeller (degrees)

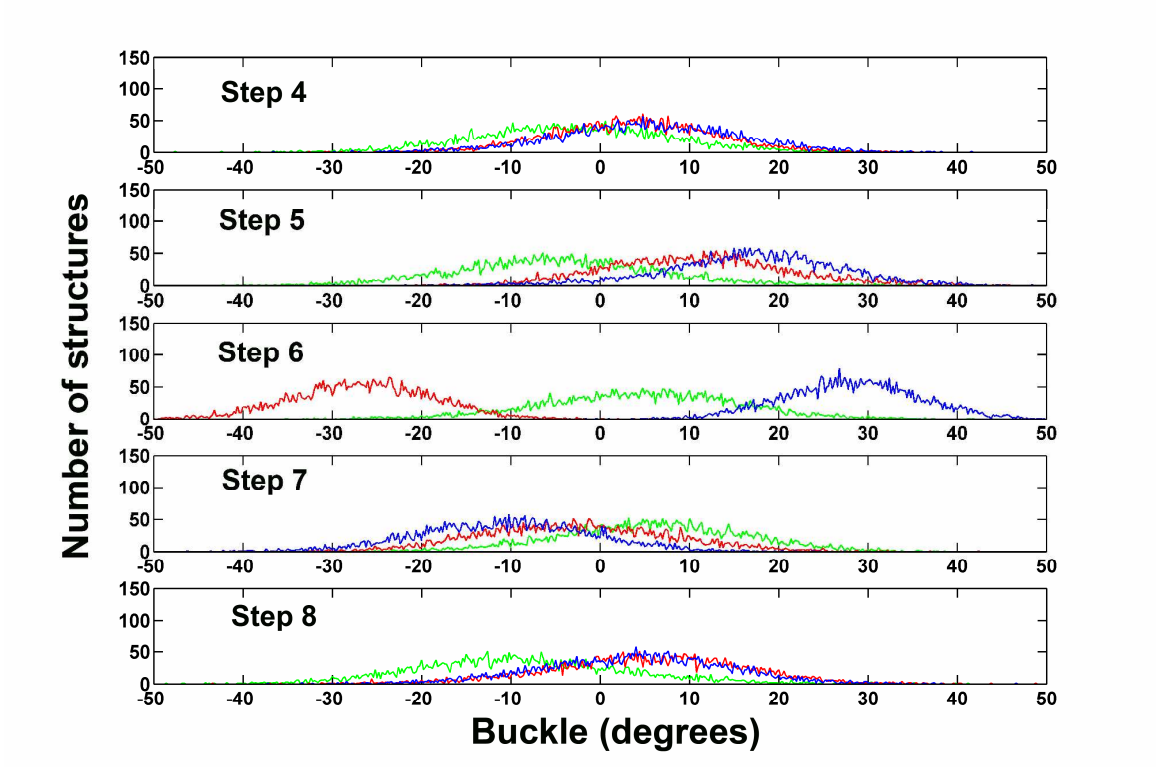


**Figure S4.** Population distributions of duplex helicoidal parameters at and surrounding the lesion site. The 14*R* (+)-adduct is red, the 14*S* (−)-adduct is blue, and the unmodified control duplex is green. Means and standard deviations are given in Table S2.

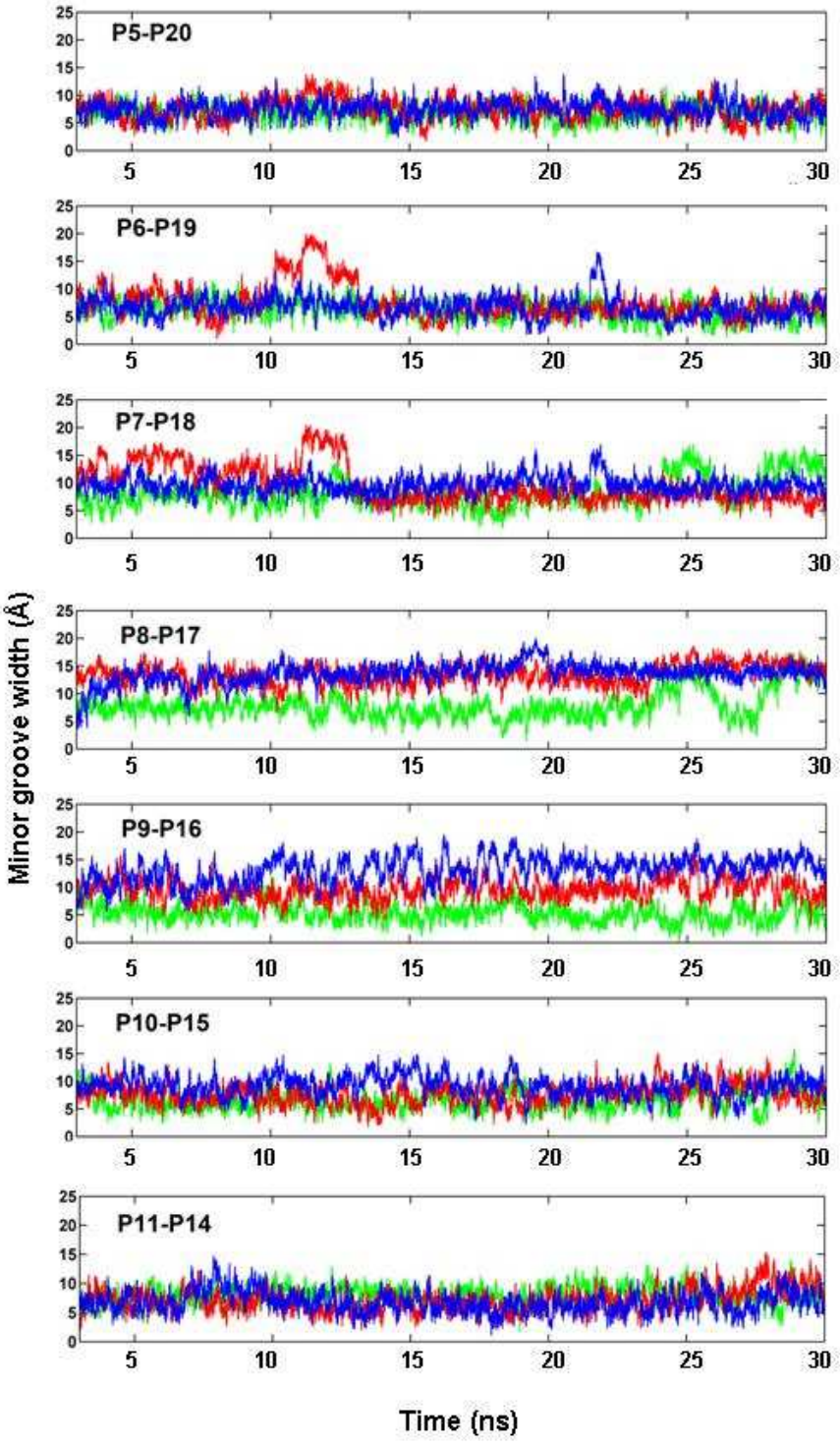
P5-P20
P6-P19
P7-P18
P8-P17
P9-P16
P10-P15
P11-P14
Minor groove width (Å)
Time (ns)

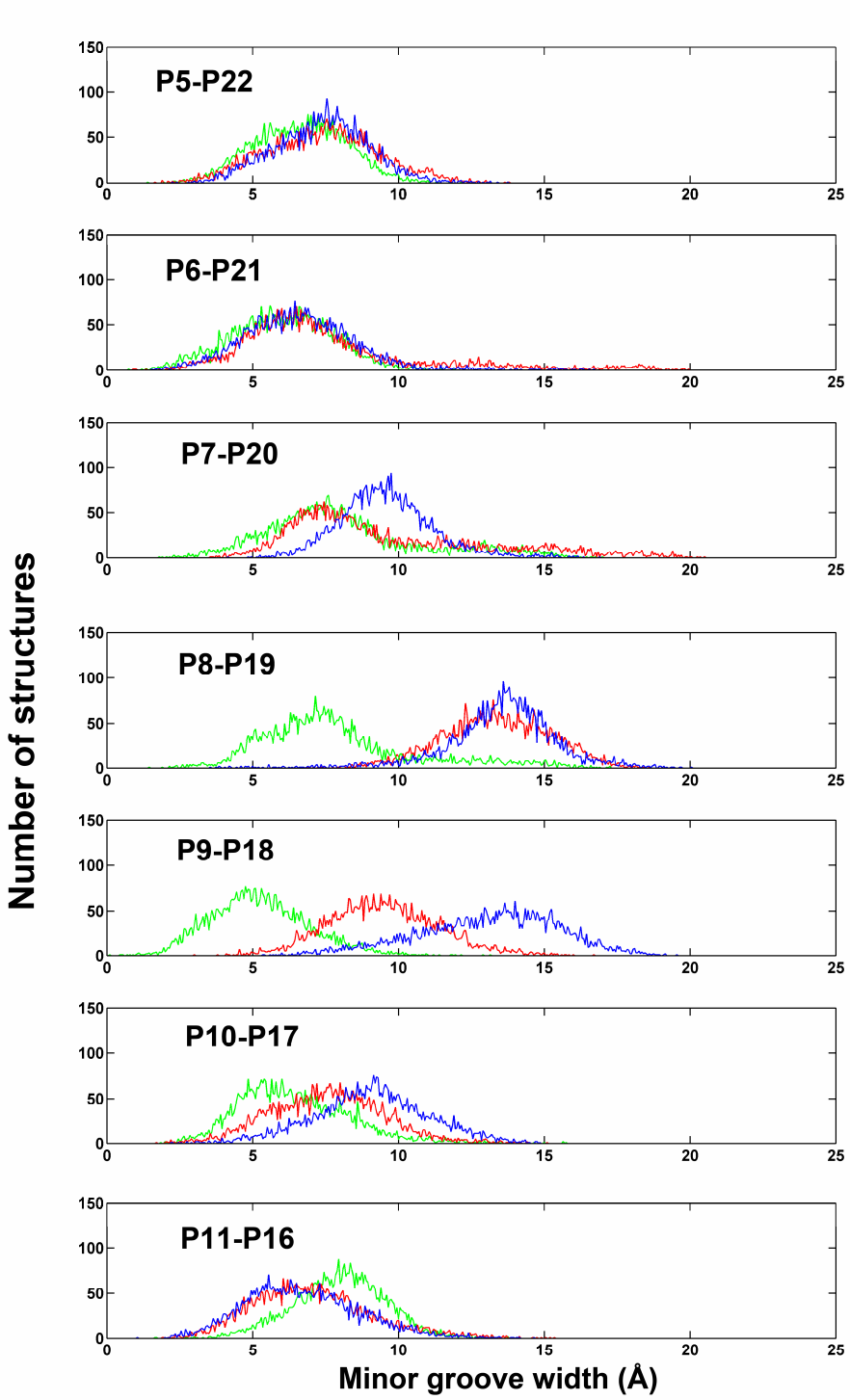


**Figure S5.** Time-dependence and population distributions of the minor groove widths. The 14*R* (+)-*trans*-*anti*-DB[*a*,*l*]P-$N^6$-dA adduct is red, the 14*S* (–)-*trans*-*anti*-DB[*a*,*l*]P-$N^6$-dA adduct is blue, and the unmodified control duplex is green. Means and standard deviations are given in Table S2.

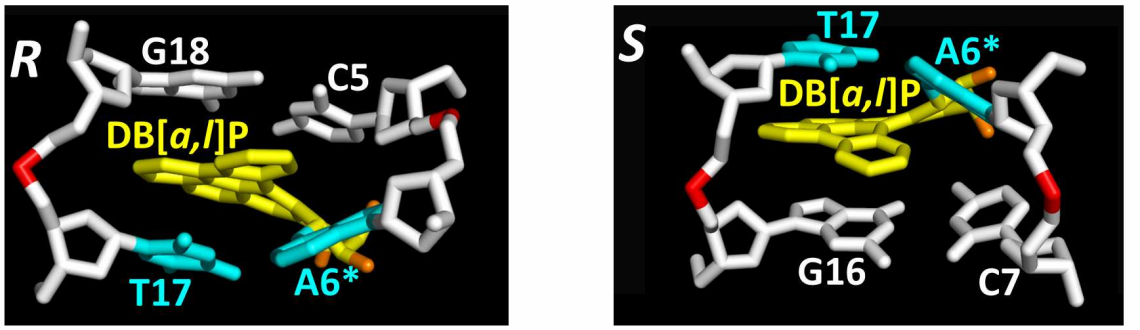


**Figure S6.** Stick views looking into the minor groove of the intercalation pocket, the ((C5-A6*)•(T17-G18) segment for the 14*R* (+)-adduct and the (A6*-C7)•(G16-T17) segment for the 14*S* (−)-adduct.

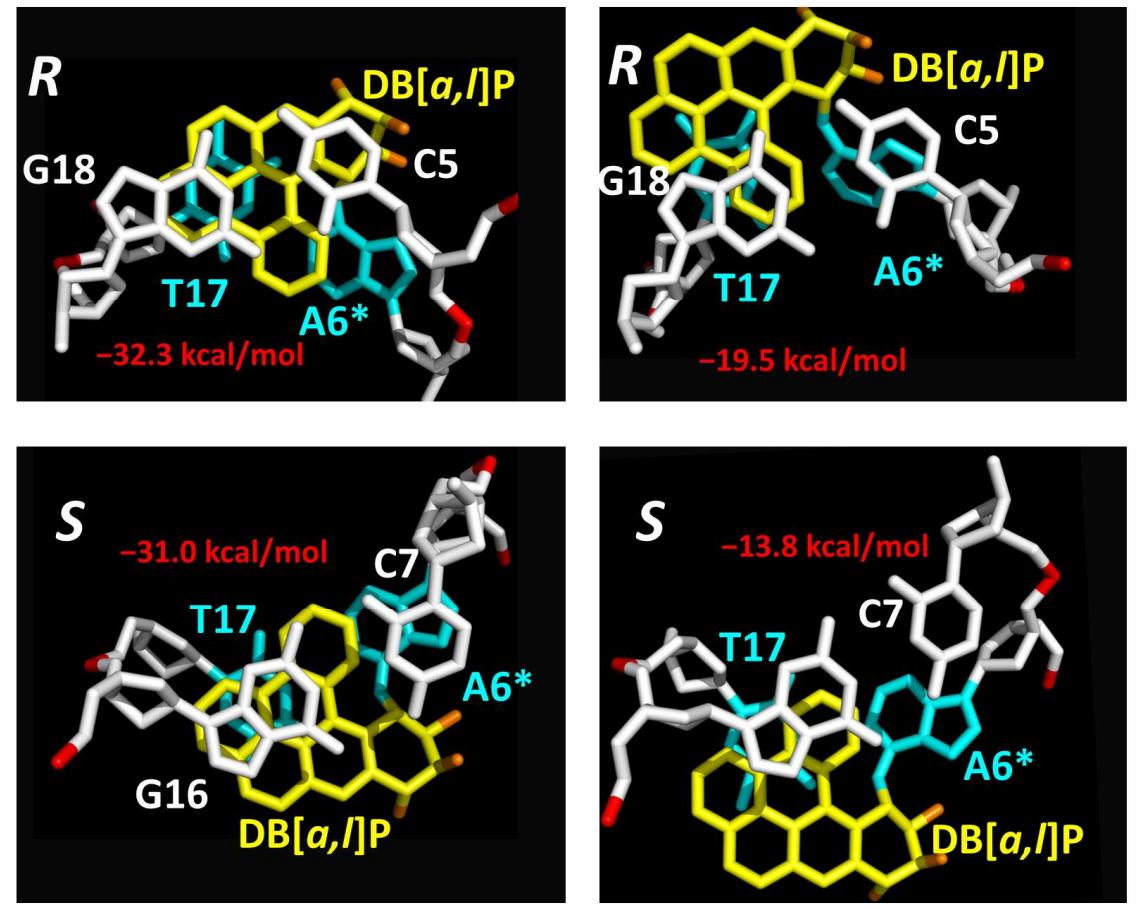


**Figure S7** Maximally and minimally stacked structures from the ensembles (*R* stereoisomer: at 9,521 ps and 6,036 ps, respectively; *S* stereoisomer: at 5,926 ps and 3,456 ps, respectively). Energies associated with these structures are given. Note that in the *S* stereoisomer, C7 is never in proximity with the DB[*a,l*]P ring system, while C5 can overlap with it in the *R* stereoisomer.

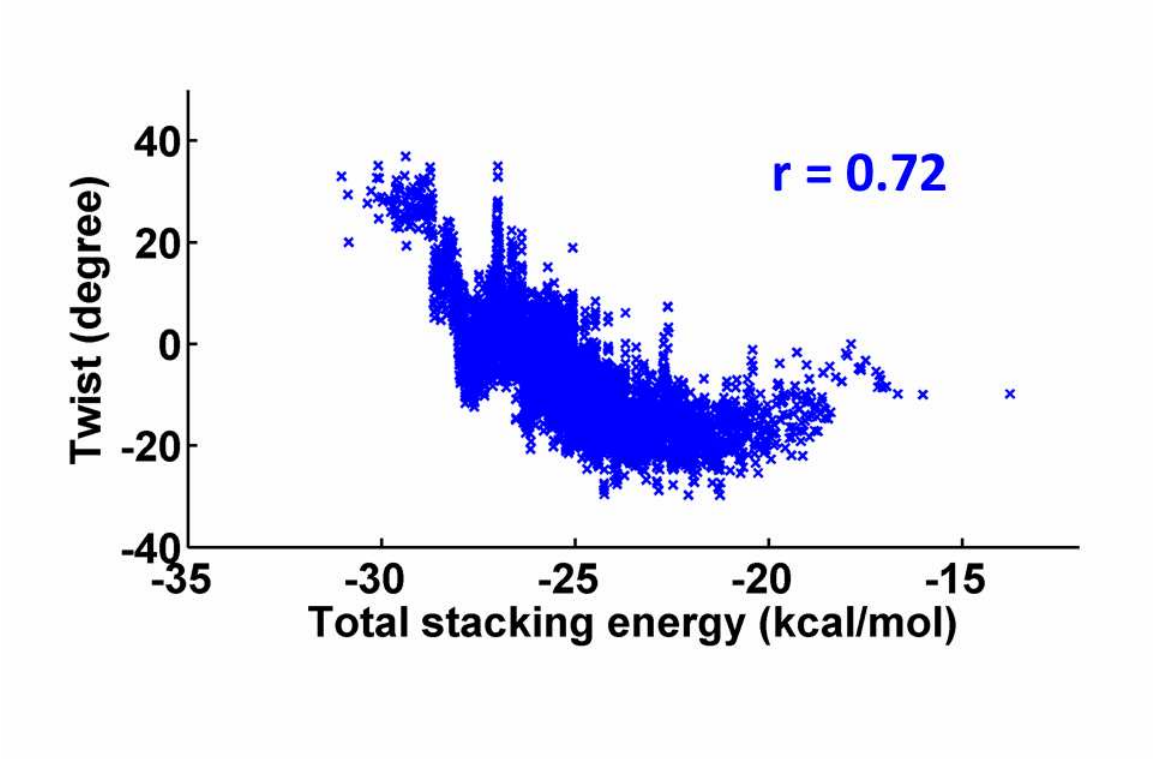


**Figure S8** Scatter plot showing the correlation between total van der Waals interaction energy in the intercalation pocket and Twist in the 14*S* (–)-*trans*-*anti*-DB[*a,l*]P-$N^2$-dA adduct. The correlation coefficient is shown.

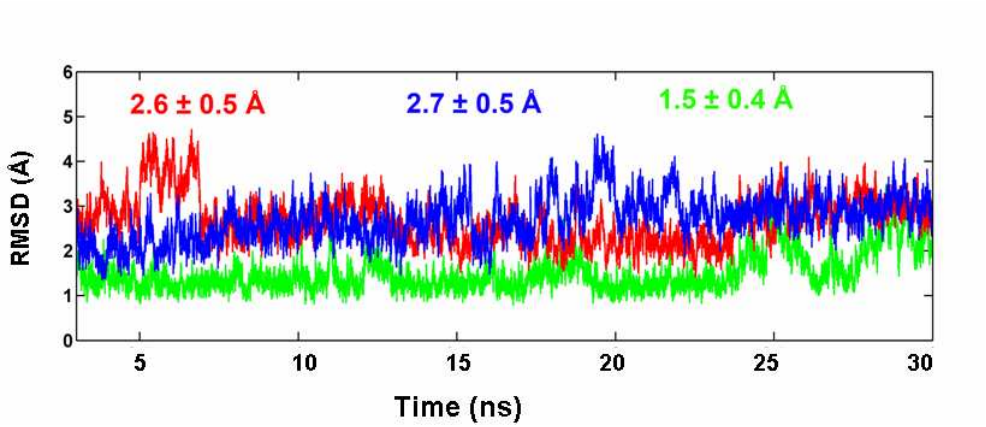


**Figure S9.** Time-dependence of RMSDs for the 14*R* (+)- (red) and 14*S* (–)-*trans*-*anti*-DB[*a*,*l*]P-$N^6$-dA (blue) adducts as well as the unmodified control duplex (green). Ensemble average values and standard deviations are given. Only the central 9-mer is considered in this analysis.

# References


1. Case, D. A., Darden, T. A., Cheatham III, T. E., Simmerling, C. L., Wang, J., Duke, R. E., Luo, R., Merz, K. M., Pearlman, D. A., Crowley, M., Walker, R. C., Zhang, W., Wang, B., Hayik, S., Roitberg, A., Seabra, G., Wong, K. F., Paesani, F., Wu, X., Brozell, S., Tsui, V., Gohlke, H., Yang, L., Tan, C., Mongan, J., Hornak, V., Cui, G., Beroza, P., Mathews, D. H., Schafmeister, C., Ross, W. S., and Kollman, P. A. (2006) AMBER 9, University of California, San Francisco, CA.
2. Jorgensen, W. L., Chandreskhar, J., Madura, J. D., Imprey, R. W., and Klein, M. L. (1983) *J. Chem. Phys. 79*, 926-935.
3. Darden, T., York, D., and Pedersen, L. (1993) *J. Chem. Phys. 98*, 10089-10092.
4. Essmann, U., Perera, L., Berkowitz, M. L., Darden, T., Lee, H., and Pederson, L. G. (1995) *J. Chem. Phys. 103*, 8577-8593.
5. Ryckaert, J. P., Ciccotti, G., and Berendsen, H. J. C. (1977) *J. Comp. Phys. 23*, 327-341.
6. Berendsen, H. J. C., Postma, J. P. M., van Gunsteren, W. F., DiNola, A., and Haak, J. R. (1984) *J. Chem. Phys. 81*, 3684-3690.
7. Simmerling, C., Elber, R., and Zhang, J. (1995), pp 241-265, Netherlands: Kluwer.
8. Hingerty, B. E., Figueroa, S., Hayden, T. L., and Broyde, S. (1989) *Biopolymers 28*, 1195-1222.
9. Saenger, W. (1983) In *Principles of Nucleic Acid Structure* p226, Springer-Verlag, New York.
10. Calladine, C. R., and Drew, H. R. (1997), Morgan Kaufmann.
11. Cosman, M., Fiala, R., Hingerty, B. E., Laryea, A., Lee, H., Harvey, R. G., Amin, S., Geacintov, N. E., Broyde, S., and Patel, D. (1993) *Biochemistry 32*, 12488-12497.
12. Cosman, M., Laryea, A., Fiala, R., Hingerty, B. E., Amin, S., Geacintov, N. E., Broyde, S., and Patel, D. J. (1995) *Biochemistry 34*, 1295-1307.